ResearchGate

See discussions, stats, and author profiles for this publication at: https://www.researchgate.net/publication/261762609

Refined OPLS All-Atom Force Field for Saturated Phosphatidylcholine Bilayers at Full Hydration

ARTICLE *in* THE JOURNAL OF PHYSICAL CHEMISTRY B · APRIL 2014

Impact Factor: 3.3 · DOI: 10.1021/jp5016627 · Source: PubMed

CITATIONS
28

READS
234

5 AUTHORS, INCLUDING:

Arkadiusz Maciejewski
Independent Research.
2 PUBLICATIONS **91** CITATIONS
SEE PROFILE

Marta Pasenkiewicz-Gierula
Jagiellonian University
88 PUBLICATIONS **2,732** CITATIONS
SEE PROFILE

Ilpo Vattulainen
Tampere University of Technology
282 PUBLICATIONS **7,852** CITATIONS
SEE PROFILE

Tomasz Róg
Tampere University of Technology
135 PUBLICATIONS **3,204** CITATIONS
SEE PROFILE

Available from: Marta Pasenkiewicz-Gierula
Retrieved on: 23 January 2016

THE JOURNAL OF PHYSICAL CHEMISTRY B

Article

pubs.acs.org/JPCB

Refined OPLS All-Atom Force Field for Saturated Phosphatidylcholine Bilayers at Full Hydration

Arkadiusz Maciejewski,[†,‡] Marta Pasenkiewicz-Gierula,[‡] Oana Cramariuc,[†] Ilpo Vattulainen,[†,§] and Tomasz Rog*[,†]

[†]Department of Physics, Tampere University of Technology, PO Box 692, FI-33101 Tampere, Finland

[‡]Faculty of Biochemistry, Biophysics and Biotechnology, Jagiellonian University, ul. Gronostajowa 7, 30-387 Kraków, Poland

[§]MEMPHYS Center for Biomembrane Physics, University of Southern Denmark, DK-5230 Odense, Denmark

Supporting Information

ABSTRACT: We report parametrization of dipalmitoyl-phosphatidylcholine (DPPC) in the framework of the Optimized Parameters for Liquid Simulations all-atom (OPLS-AA) force field. We chose DPPC as it is one of the most studied phospholipid species and thus has plenty of experimental data necessary for model validation, and it is also one of the highly important and abundant lipid types, e.g., in lung surfactant. Overall, PCs have not been previously parametrized in the OPLS-AA force field; thus, there is a need to derive its bonding and nonbonding parameters for both the polar and nonpolar parts of the molecule. In the present study, we determined the parameters for torsion angles in the phosphatidylcholine and glycerol moieties and in the acyl chains, as well the partial atomic charges. In these calculations, we used three methods: (1) Hartree−Fock (HF), (2) second order Møller−Plesset perturbation theory (MP2), and (3) density functional theory (DFT). We also tested the effect of the polar environment by using the polarizable continuum model (PCM), and for acyl chains the van der Waals parameters were also adjusted. In effect, six parameter sets were generated and tested on a DPPC bilayer. Out of these six sets, only one was found to be able to satisfactorily reproduce experimental data for the lipid bilayer. The successful DPPC model was obtained from MP2 calculations in an implicit polar environment (PCM).

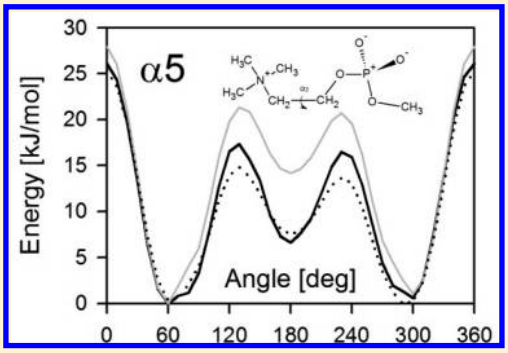

1. INTRODUCTION

Lipids comprise a large class of biomolecules that are basic constituents of biomembranes. Together with proteins and carbohydrates, lipids play fundamental roles in biomembrane function, maintaining cell integrity, protecting the cell from its environment, separating intracellular compartments, and receiving and transducing signals necessary for the cell function.[1]

The most prevalent lipid type that forms eukaryotic cell membranes is phosphatidylcholine (PC). It consists of four structural elements: the phosphatidylcholine moiety, glycerol backbone, and two acyl chains. The glycerol backbone is the key fragment to which the three others are attached (Figure 1). The phosphatidylcholine moiety (alpha, α-chain) is linked to the glycerol carbon atom C1 (*sn*-3 position), and the acyl chains are attached to C2 (*sn*-2 position; beta, β-chain) and C3 (*sn*-1 position; gamma, γ-chain) carbon atoms. Figure 1 shows the chemical structure of a typical PC molecule with all structural elements and torsion angles marked according to the Sundaralingam's nomenclature (with an exception for the C1 and C3 carbon atoms that are here swapped).[2]

The atomistic molecular dynamics (MD) simulation technique has become a versatile computational method that is widely used in studies of lipid membranes. Motivated by the profound added value that molecular simulations have conferred to experimental science, increasingly effort is being invested in developing and improving parametrizations of models for complex biomolecular systems. Validation of these models starts with the comparison of the lipid bilayer's phase behavior against experimental observations. This is followed by considering other membrane properties that affect a variety of observables. One such example is to calculate the surface area per lipid and the hydrocarbon chain order parameter since these govern various dynamical membrane properties such as lateral diffusion and permeation.

Overall, these bilayer properties are sufficiently well reproduced by several older united-atom force fields (where apolar hydrogen atoms are not explicitly included).[3−8] The most recent of these united-atom force fields is an extension of the TraPPE (Transferable Potentials for phase Equilibria) force field, which has parameters for a large number of lipid classes, such as PC, phosphatidylethanolamine (PE), phosphatidylserine (PS), and phosphatidylglycerol (PG).[9] Lipid bilayers parametrized with this systematically derived set of parameters

Received: February 16, 2014
Revised: April 8, 2014
Published: April 8, 2014

 © 2014 American Chemical Society dx.doi.org/10.1021/jp5016627 | *J. Phys. Chem. B* 2014, 118, 4571−4581

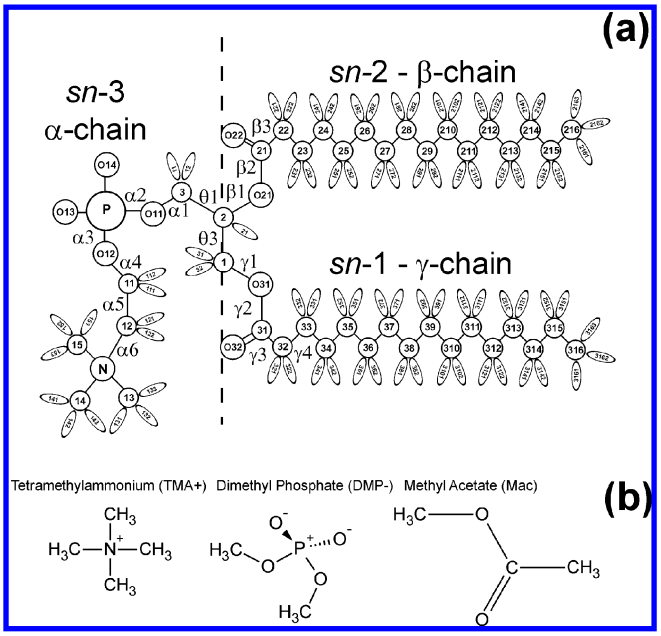

Figure 1. (a) Chemical structure of the DPPC molecule together with atom numbering and notation used for the recalculated torsion angles, according to Sundaralingam's nomenclature (with an exception for C1 and C3 carbon atoms that are swapped), and (b) chemical structures of the molecular fragments used for calculations of partial atomic charges.

provide results that are in good agreement with experimental data.

Meanwhile, there is reason to ask whether united-atom models are appropriate to consider questions where atomistic features are important, such as in permeation across membranes, binding of lipids to their binding pockets in membrane proteins, and considerations of glycomolecules where all the structural details may be profoundly important. Quite often the use of united-atom models is justified based on their computational efficiency, but given that computational resources are getting better all the time, this justification may not be relevant in all the cases.

Consequently, all-atom simulation models (with all hydrogens explicitly present) have recently become more and more popular to consider research themes where the atomistic details can be expected to be truly important. The strength of all-atom models lies in their detailed nature, but this implies that the requirements to derive excellent all-atom models that would be fully consistent with experimental data are also more stringent compared to united-atom descriptions. This issue has also been realized in practice: in contrast to united-atom force fields, older all-atom force fields have often underestimated the surface area per lipid. One of such force fields is CHARMM. Originally, models of bilayers made up of saturated PCs parametrized in the CHARMM force field incorrectly reproduced both the thermotropic bilayer phases and the surface area per PC. Therefore, bilayers had to be simulated under constant surface tension,[10] which biologically is not appropriate since biological membranes are expected to be tensionless. However, reparameterization of the partial atomic charges on the PC headgroup improved both the phase state and the area per PC in bilayers consisting of various PC molecules.[11,12] Subsequent rigorous recalculation of the CHARMM lipid parameters led to a new CHARMM 36 force field that includes parameters for DPPC, DMPC, DLPC, POPC, DOPC, polyunsaturated phospholipids, as well as cholesterol.[13−15] Moving on, the necessity to include surface tension in MD simulations of PC bilayers to properly reproduce experimental data applies also to the General Amber force field[16,17] and to the Amber force field for lipids, called Lipid11.[18] Simulations of tensionless lipid bilayers became possible in the newest version of Amber lipids, called Lipid14.[19] Meanwhile, a new force field, called Slipids, which also uses the Amber potential energy function, reproduces quite a few properties of bilayers consisting of different types of lipids.[20−22]

Two other important areas of force field development include coarse-grained models and atomic polarizability (polarizable force fields). Coarse-grained (CG) models of lipids, in which a group of atoms is replaced by a single bead, have been under considerable development during the past decade.[23,24] Especially popular are models of lipids and other biomolecules parametrized in the context of the MARTINI description:[25] The molecular descriptions and force fields consistent with this model have been successfully used in numerous studies of, e.g., lipid bilayer phase transitions,[26] domain formation in lipid mixtures,[27] membrane protein aggregation and dynamics,[28,29] lipoproteins,[30−32] and technologically relevant polymer systems.[33,34] Meanwhile, the progress in the atomistic regime has been somewhat more complicated, since the development of polarizable force fields that would be both highly accurate and computationally efficient is a quest that is not among the simple ones. To the best of our knowledge, only a couple of polarizable force fields for lipids have been developed so far—one uses the polarizable charge equilibration approach[35−37] and the other is based on the classical Drude oscillator.[38] Yet, progress is being made; for instance, effects of polarizability on the free energy of transfer of a water molecule into the bilayer interior were recently shown in ref 39. Nevertheless, the downside of polarizable force fields is their computational cost that is quite profound compared to standard (nonpolarizable) atomistic force fields, the difference typically being an order of magnitude in computational cost. Obviously, for practical reasons, the motivation to improve existing nonpolarizable all-atom force fields for biomolecular simulations is high.

In this paper, we present recalculated torsional parameters, partial atomic charges, and van der Waals (vdW) parameters for the polar and hydrocarbon parts of PC molecules (headgroup, glycerol backbone, acyl chain region). The parametrization that we discuss here is compatible with the Optimized Parameters for Liquid Simulations all-atom (OPLS-AA) force field, that was originally developed by Jorgensen et al.[40] OPLS-AA includes a large set of parameters for proteins,[41,42] nucleic acids,[43] and carbohydrates,[44] as well as various drug molecules.[45−48] However, up to now, lipids have not been fully parametrized in this force field. Only parts of the molecules including long hydrocarbons,[49] *n*-pentadecane, methyl acetate, and dimethyl phosphate anion were reparameterized.[50]

In our previous MD simulation studies of phospholipid bilayers, we used the OPLS force field for both the united-atom[51,52] and all-atom[53−55] models. These simulations revealed certain discrepancies between our models and experimental data, as well as recent QM calculations,[56] and this has given us motivation for the improvement of the OPLS-AA parametrization for phospholipids. As shown below, the reparameterization does not increase the computational load, but it

dx.doi.org/10.1021/jp5016627 | J. Phys. Chem. B 2014, 118, 4571−4581

significantly improves the accuracy of the OPLS-AA description.

2. METHODS

In the present work, we developed a computer model for the phosphatidylcholine (PC) molecule compatible with the OPLS-AA force field. The derivation of the model was carried out through recalculation of the force field parameters that focused on the polar part of the molecule, though the acyl chain region was also considered for the sake of completeness. The newly derived parameters include partial atomic charges, torsional parameters, and in some cases also van der Waals (vdW) parameters. The bond stretching and angle bending parameters were adopted from the BOSS-4.8 database.[40] Scaling factors for the 1−4 interactions were set the same as in OPLS (0.5 for both electrostatic and vdW interactions). For water, we employed the TIP3P model, which is compatible with the OPLS force field.[57] All MD test simulations of the bilayers built of PCs parametrized with the new force field parameters were performed with the GROMACS 4 package.[58] We employed several approaches for the derivation of the PC molecule parameters and obtained six parameter sets that were subsequently subjected to tests. Of these six sets, only one turned out to fully reproduce the experimental values for the representative bilayer properties.

2.1. Electronic Structure Calculations. *2.1.1. Computational Methods.* Geometry optimizations were carried out first at the Hartree−Fock (HF) level by employing a moderately sized polarized basis set 6-31G*. The HF structures were further optimized using second order Møller-Plessent perturbation theory (MP2) with the 6-31G** basis set and also the Density Functional Theory (DFT), by employing the same basis set and the B3LYP functional.[59] Ultrafine grid spacing was imposed in the DFT calculations in order to improve the reliability of the results.

The basis set was further augmented with diffuse functions (6-31+G**) for the calculations involving an anionic group. In larger molecules used in dihedral potential calculations (see insets to Figures 3 and 4), diffuse functions were only used on phosphorus and nonester oxygen atoms due to "basis-set linear dependence problems" common in variational methods (HF and MP2).[60] In these calculations, we used Cartesian *d*-functions instead of the default spherical harmonic components for the polarization functions. All electronic structure calculations were carried out using the Gaussian-03/09 suite.[61]

2.1.2. Headgroup Partial Atomic Charges. The polar part of the PC molecule was divided into three smaller units: tetramethylammonium (TMA+), dimethyl phosphate anion (DMP-), and methyl acetate (MAc) (Figure 1b). The geometries of TMA+, DMP−, and MAc were optimized according to their point group symmetries (T_D, C_2, and C_s, respectively). Tight convergence criteria were imposed during geometry optimization, i.e., the maximum force acting on an atom in the system and the root-mean-square (RMS) of the forces were below 1.5×10^{-5} and 1.0×10^{-5} Hartree/Bohr, respectively. At the same time, the maximum structural change of one coordinate, as well as the average RMS change over all structural parameters, had values below 6.0×10^{-5} and 4.0×10^{-5}, respectively.

Presented here, calculations of partial atomic charges were carried out in a vacuum and in a polar environment. The effects of a polar solvent were included implicitly by employing the polarizable continuum model[62] (PCM) as implemented in the Gaussian package. In the MP2 calculations, we first computed the solvent effect on the standard self-consistent field (SCF) density and then at MP2 level. Additionally, DFT calculations were also performed both in vacuum and in an implicit solvent. The computational details for all HF, MP2, and DFT calculations are described in Section 2.1.1. Including solvent effects in the development of force fields is not a new idea. For example, PCM was used in the Slipids[20] development, and implicit solvent models have been used to obtain the Amber force field.[63,64] The CHARMM procedure of deriving partial charges by optimizing them to reproduce interaction energies with water seems to play a similar role. Calculations of ionization energies of phosphate ions have shown that the use of PCM dramatically improves the agreement between experimentally measured and computed energies[65] due to accounting for polarization.

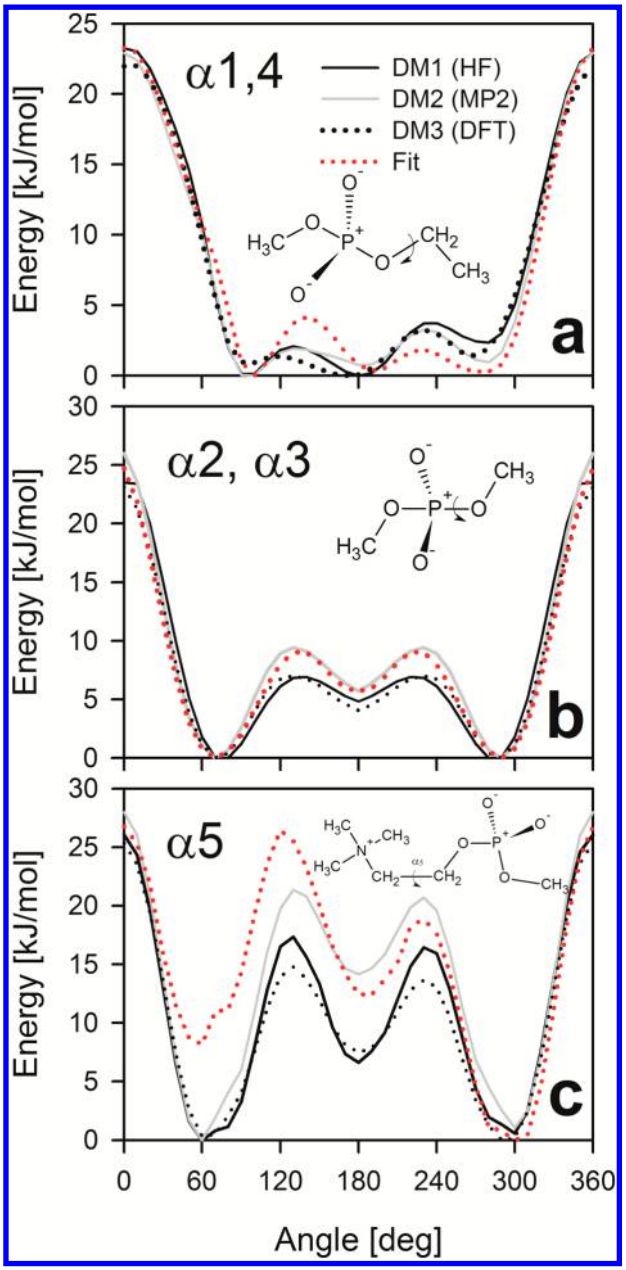

Figure 2. Profiles of torsional energy for the α-chain torsion angles. Molecular fragments used for calculations are shown in the inset.

dx.doi.org/10.1021/jp5016627 | J. Phys. Chem. B 2014, 118, 4571−4581

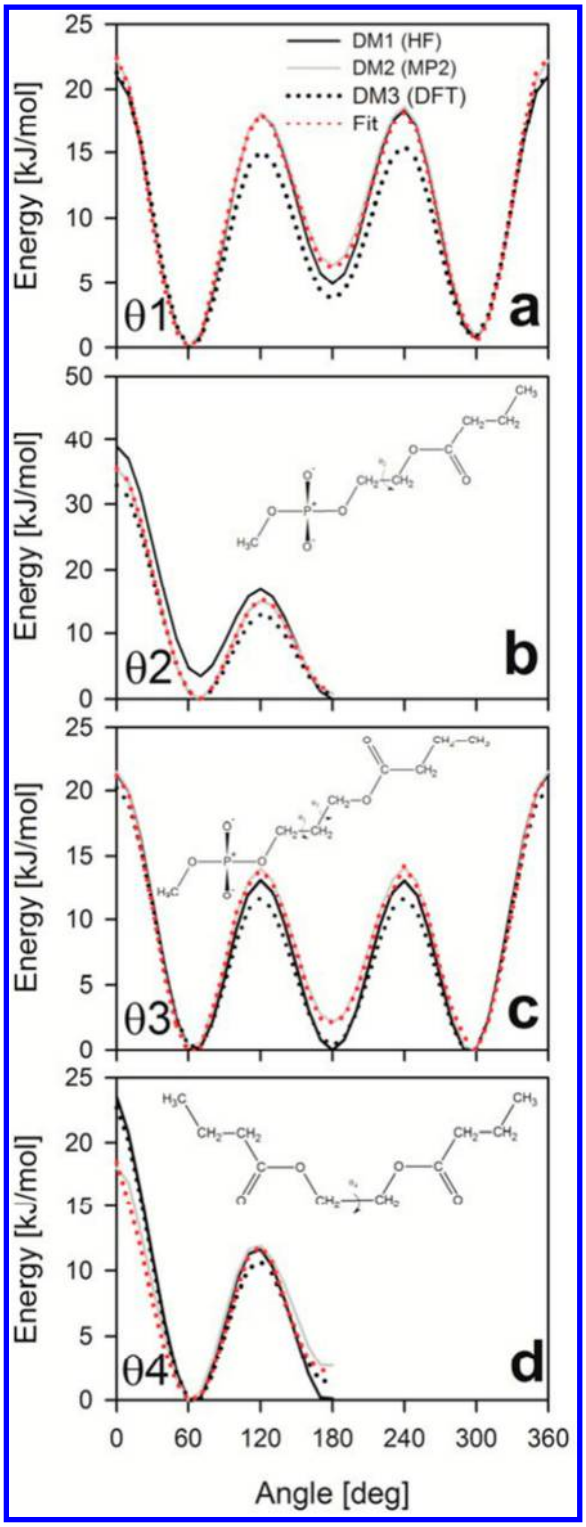

Figure 3. Profiles of torsional energy for the θ-chain torsion angles. Molecular fragments used for calculations are shown in the inset. For $\theta 1$ and $\theta 3$, the same fragment was used.

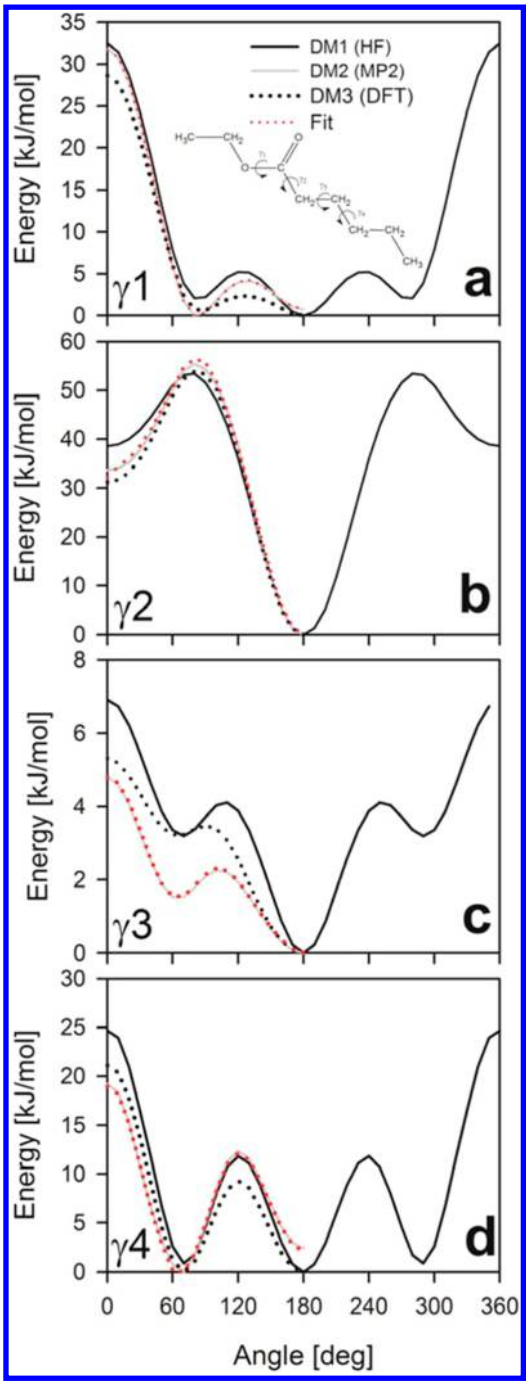

Figure 4. Profiles of torsional energy for the γ-chain torsion angles. Molecular fragments used for calculations are shown in the inset of panel a.

The fitting of the partial atomic charges to the electrostatic potential calculated at HF, MP2, and DFT levels was done by employing the ChelpG algorithm.[66] The classical Coulomb energy function was fitted to the calculated potential values to obtain partial atomic charges in two stages. During the first stage, weak hyperbolic restraints (5.0×10^{-4}) were used for the heavy atoms. During the second stage, heavier hyperbolic restraints (1.0×10^{-3}) were applied only to the carbon atoms of the methyl ($-CH_3$) and methylene ($-CH_2$) groups. Symmetrically identical atoms/groups within the molecule were treated as equivalent. An additional restraint was imposed to ensure that the partial atomic charges sum up to the formal charge of the molecule. The fitting procedure was accomplished with the R.E.D. IV interface[67] with the RESP program.[68,69]

2.1.3. Headgroup Dihedral Potentials. In these calculations, the polar part of the PC molecule was divided into seven representative fragments. Each fragment contained at least one dihedral angle to be adjusted. The chemical structures of the fragments are shown in Figures 2 and 4.

dx.doi.org/10.1021/jp5016627 | J. Phys. Chem. B 2014, 118, 4571−4581

The total potential energy profile for the rotation of a given dihedral angle in the PC polar part was sampled by successive QM structure optimizations in vacuum, except for $\alpha 5$ (see Figure 1 and Table 2), for which the optimization was performed in a polar environment (PCM model).[62] The HF, MP2, and DFT calculations were performed as described in Section 2.1.1, and the QM energy was calculated for dihedral angles (active coordinate) at 10° intervals in the range 0−360°, or 0−180° in the case of more computationally demanding scans that were rotationally symmetric. At each step, the remaining internal degrees of freedom were allowed to relax during the energy minimization procedure.

In the next step, a similar procedure was employed while performing molecular mechanics (MM) calculations with the torsion potential for the active coordinate set to zero. A restraining force constant was adjusted such that it allowed, at most, a ±1.5° deviation from the desired value of the sampled dihedral angle. Because restraints contribute to the evaluated potential energy, postscans were needed to reevaluate the total potential energy without imposed restraints. As a result, the profile of the total MM potential energy, without an energetic contribution from the active dihedral, was derived.

The torsion potential energy profile is a function of a single torsion angle ϕ, but a few quadruple pairs differing by phase shifts are possible. The functional form reproducing the profile adopted in GROMACS is the sum of the first five terms of the cosine power series, the so-called Ryckaert-Bellemans (RB) dihedral potential, and is given in eq 1:

$$V_{rb}(\phi_{ijkl}) = \sum_{n=0}^{5} C_n(\cos(\Psi))^n \quad (1)$$

where $\psi = \phi - 180°$. During fitting, the polymer convention was adopted ($\psi_{trans} = 0$). The RB coefficients C_n in eq 1 were found by minimizing the least-squares function of the differences between the QM and MM total potential energies and the corresponding Ryckaert-Bellemans potential values. In this process, the Nonlinear Least Squares Marquardt−Levenberg algorithm[70] implemented in Gnuplot[71] was used.

2.1.4. Hydrocarbon Chain Parameterization. New parameters for hydrocarbon chains were calculated for three hydrocarbons of length 6-, 10-, and 14-carbon atoms. Both dihedral potentials and vdW parameters were calculated, while bond stretching, angle bending, and partial atomic charges were the ones in the original OPLS-AA force field. The procedure to obtain dihedral potential parameters was similar to that already presented above with the main difference being the evaluation of the QM potential energy. Here, the Hybrid Methods for Interaction Energies (HM-IE) method was used for accurate but efficient energy evaluation.[72,73] The potential energies were calculated for the central torsion angle of each hydrocarbon. The calculations were performed in three steps. First, the geometry of the hydrocarbon molecule was optimized at MP2/cc-pVDZ level; the minimum energy obtained in this way is denoted MP2/SBS (Small Basis Set). Second, two total energies for the optimized structure were calculated, one using CCSD(T)/DZ, denoted CCSD(T)/SBS, and the other using MP2/cc-pVTZ, denoted MP2/LBS (Large Basis Set). Finally, the required total potential energy was estimated using eq 1 in ref 72. While fitting the new RB coefficients, the selected atoms were four consecutive carbon atoms (C−C−C−C). The RB coefficients for the remaining sets of the four atoms (C−C−C−H and H−C−C−H) associated with the same dihedral were the standard RB coefficients adopted from the BOSS-4.8 database. The final stage of a hydrocarbon parametrization was to test several combinations of sigma and epsilon parameters of the vdW potential and adjust to the RB coefficients of the C−C−C−C torsion term.

2.2. Classical Molecular Dynamics Simulations. *2.2.1. Simulated Models.* In this work, we tested the six sets of parameters derived from HF, DFT, and MP2 calculations that are summarized in Table 3. The primary system studied in these tests was a lipid bilayer consisting of dipalmitoylphosphatidylcholine (DPPC), one of the most studied saturated phosphatidylcholines. The bilayer comprised 128 lipid and 3500 water molecules. The initial structures of the bilayers originated from our previous studies.[74] We also simulated pure hydrocarbons of varying chain lengths to derive

Table 1. Variants of Partial Atomic Charge Sets Investigated in the Present Study

	TMA+	DMP−	CF3
CM1v	HF/6-31G* Vacuum	HF/6-31G* Vacuum	HF/6-31G* Vacuum
CM1w	HF/6-31G* Water (PCM)	HF/6-31G* Water (PCM)	HF/6-31G* Water (PCM)
CM2v	MP2/6-31G** Vacuum	MP2/6-31+G**//6-31G**_Dyf_PO2 Vacuum	MP2/6-31G** Vacuum
CM2w	MP2/6-31G** Water (PCM)	MP2/6-31+G**//6-31G**_Dyf_PO2 Water (PCM)	MP2/6-31G** Water (PCM)
CM3v	B3LYPAug-cc-pVTZ//6-31G** Vacuum	B3LYP/Aug-cc-pVTZ//6-31+G** Vacuum	B3LYP/Aug-cc-pVTZ//6-31G** Vacuum
CM3w	B3LYP/6-31G** Water (PCM)	B3LYP/6-31+G** Water (PCM)	B3LYP/6-31G** Water (PCM)

Table 2. Variants of Dihedral Potential Models Explored in This Study

dihedral model	method	solvation	dihedral
DM1	HF/6-31G**	Vacuum	α = 1, 2, 3, 4; γ = 1, 2, 3, 4; θ = 1, 2, 3, 4
		Water (PCM)	α-5
DM2	MP2/6-31G**_Dyf_PO2	Vacuum	α = 1, 2, 3, 4; γ = 1, 2, 3, 4; θ = 1, 2, 3, 4
		Water (PCM)	α-5
DM3	B3LYP/6-31G**_Dyf_PO2	Vacuum	α = 1, 2, 3, 4; γ = 1, 2, 3, 4; θ = 1, 2, 3, 4
		Water (PCM)	α-5

Table 3. Summary of the Force Field Models Tested in This Paper

bilayer system	model shortcut dihedrals/charges	dihedral model	charge model
B1	HF/HF_vac	DM1	CM1v
B2	HF/HF_wat	DM1	CM1w
B3	MP2/MP2_vac	DM2	CM2v
B4	**MP2/MP2_wat**	**DM2**	**CM2w**
B5	MP2/DFT_vac	DM3	CM3v
B6	DFT_wat	DM3	CM3w

dx.doi.org/10.1021/jp5016627 | J. Phys. Chem. B 2014, 118, 4571−4581

Table 4. Partial Charges and Atom Types Used in Headgroup Parameterization[a]

		partial charge					
atom indexes	atom type	CM1v HF	CM1w HF	CM2v MP2	CM2w MP2	CM3v DFT	CM3w DFT
1, 5, 9	CN3	−0.2600	−0.272	−0.2636	**-0.2795**	−0.2173	−0.2576
2, 3, 4, 6, 7, 8, 10, 11, 12	HCN	0.1462	0.1445	0.1497	**0.1484**	0.1441	0.1433
13	N3C	0.2856	0.354	0.2580	**0.3372**	0.1400	0.3109
14	*CT*	−0.1138	−0.1275	−0.1139	**-0.1311**	−0.0732	−0.1143
15, 16	*HC*	0.1462	0.1445	0.1497	**0.1484**	0.1441	0.1433
17, 25	*CT*	0.2005	0.2350	0.2282	**0.2654**	0.1943	0.2793
18, 19, 26, 27	*HC*	−0.0053	0.0184	−0.0134	**0.0161**	0.0302	−0.0003
20, 24	OSP/*OS*	−0.5514	−0.5671	−0.5781	**-0.6096**	−0.4758	−0.5769
21, 22	O2P	−0.8427	−0.8955	−0.8890	**-0.9666**	−0.784	−0.8946
23	*P*	1.4084	1.3816	1.5314	**1.5572**	1.2518	1.3856
28	*CT*	0.2175	0.2530	0.2144	**0.2496**	0.1863	0.2132
29	*HC*	0.0518	0.0467	0.0548	**0.0500**	0.0497	0.0501
30, 82	OSA/*OS*	−0.4934	−0.5124	−0.4882	**-0.5083**	−0.4171	−0.4171
31, 83	CLL/*C*	0.9644	1.0145	0.9325	**0.9766**	0.8412	0.8174
32, 84	OLL/*O*	−0.6380	−0.7014	−0.6271	**-0.6887**	−0.5722	−0.5883
33, 85	CL2	−0.3811	−0.4236	−0.3786	**-0.4104**	−0.3557	−0.3881
34, 35, 86, 87	HLC	0.1394	0.1616	0.1461	**0.1656**	0.1339	0.1564

[a]Atom indexes are shown in Figure 1 in red and can be found in the topology files in SI. Charges used in the final model validation are given in bold.

vdW parameters for PC acyl chains (details described in Section 3.2.2).

2.2.2. Simulation Protocol. The vdW interactions were cut off at 10 Å. Dispersion corrections for both energy and pressure were used in order to remove dependencies on the cutoff length and to keep the model compatible with the OPLS-AA force field. The electrostatic interactions were evaluated using the particle-mesh Ewald (PME) summation[75] with a real space cutoff of 10 Å, β-spline interpolation order of 6, and direct sum tolerance of 10^{-6}. This treatment of nonbonded interactions is recommended for all simulations employing parameters derived in this work, which, on the other hand, is compatible with the treatment of nonbonded interactions in the OPLS-AA force field.

In the real space, periodic boundary conditions in three directions and the usual minimum image convention were used. The LINCS algorithm[76] was applied to preserve the lengths of all covalent bonds in the systems, and the time step was set to 2 fs. Simulations were carried out in the isobaric−isothermal ensemble (1 atm) with a semi-isotropic pressure control and system temperature of 323 K. The temperature and pressure were controlled using the Nosé−Hoover[77,78] and the Parrinello−Rahman[79] algorithms, respectively. The temperatures of the solute and solvent were controlled independently. The list of nonbonded pairs was updated every 10 steps.

3. RESULTS

3.1. Headgroup Parameterization. *3.1.1. Nonbonding Parameters.* The partial atomic charges on the polar part of the PC molecule calculated using six different approaches (cf. Sections 2.1.1 and 2.1.2; Table 1), together with the corresponding atom types, are provided in Table 4. The atom indexes are given according to the topology files (see Supporting Information). Initially, all atom types were the same as those in the original OPLS-AA force field; however, to ensure compatibility, four new atom types were introduced. The new atom types have the same vdW parameters as those already existing in the OPLS-AA, but their torsional parameters derived in this study are different. The new types OSp and OSa are equivalent to OS (ether oxygen), and CLL and OLL are equivalent to C (carbonyl carbon) and O (carbonyl oxygen), respectively.

3.1.2. Torsion Angle Parameters. The largest effort in the present study was dedicated to the reparameterization of the torsion potentials for the torsion angles in the PC headgroup. This was necessary since some crucial parameters were either missing in OPLS-AA or derived for small molecules not relevant for PC. The torsion potential energy profiles obtained by us are shown in Figures 2 and 4, and the RB coefficients are given in Supporting Information in the GROMACS format. The calculated profiles are also provided in numerical format (Supporting Information) for use by other force-field developers. In several cases, profiles obtained for different partial atomic charge sets differ significantly in the barrier heights, as well as in energy differences between the stable conformations. These differences are large enough to affect the quality of the lipid bilayer models.

The torsional profiles for the torsion angles in the α-chain (phosphatidylcholine moiety) are shown in Figure 2. Among these angles, α5 was not parametrized in the original OPLS. Therefore, MD simulations generally used the default parameters for the assumed *trans* conformation of this angle. However, experimental data suggest that the conformation of this angle is mostly *gauche*.[80] Our calculations (Figure 2) also predict the *gauche* conformation. Torsional profiles for θ torsion angles (glycerol moiety) are shown in Figure 3, and the torsional profiles for the first four torsion angles in the γ-chain (γ1−4) are given in Figure 4. We used the same parameters for the torsion angles β1−4 as for the γ1−4 torsions.

3.2. Hydrocarbon Parameterization. The use of the original OPLS-AA parameters leads to the crystallization of long hydrocarbons (starting from dodecane) during MD simulation at temperatures above the main phase transition temperature. Consequently, the reparameterization of the PC acyl chains is clearly needed. A solution to this problem was obtained in two steps. The first step was reparametrization of the torsion potentials for hydrocarbons, and the second one was the adjustment of their vdW parameters. In a recently published paper, Siu et al. recalculated OPLS-AA parameters

dx.doi.org/10.1021/jp5016627 | J. Phys. Chem. B 2014, 118, 4571−4581

for long hydrocarbon chains;[49] however, when we started this work these parameters were not yet available.

3.2.1. Torsion Angle Parameters. Figure 5 depicts torsional energy profiles for the middle torsion angle in a hydrocarbon chain derived for 6-, 10-, and 14-carbon chains. Computations were performed at the HF and MP2 levels of theory. As can be seen from Figure 5, profiles obtained for HF are characterized by a higher barrier between the *trans* and *gauche* conformations and a greater difference in energies of both conformations. The dissimilarities between the profiles were previously described in the literature and were accounted for in, for example, the CHARMM,[10] GROMOS,[6] and Slipids[20] force fields. Figure 5 also shows that there is no difference in the profiles for chains from 6- to 14-carbon atoms obtained when a given method (HF or MP2) is used.

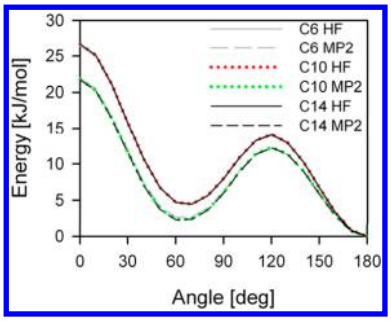

Figure 5. Profiles of torsional energy obtained in HF and MP2 calculations for hydrocarbons of length 6 (gray), 10 (red, green), and 14 (black).

3.2.2. van der Waals Parameters. In order to derive vdW parameters for PC acyl chains, we performed a series of MD simulations of boxes containing 576, 384, and 288 molecules of 8-, 12-, and 16-carbon atom hydrocarbons, respectively, with the new torsion parameters. The simulation protocol was the same as described in Section 2.2.1, and the temperature was 298 K. During these simulations, the vdW parameters were adjusted stepwise so as to reproduce the known densities and heats of vaporization of the hydrocarbons. This is the standard procedure to derive vdW parameters within the OPLS framework. The optimum performance (i.e., best agreement with experimental values) was obtained with σ = 0.3376 nm and ε = 0.276 144 kJ/mol for the carbon atom and σ = 0.2468 nm and ε = 0.125 52 kJ/mol for the hydrogen atom. The final values of the densities and heats of vaporization for the studied hydrocarbons obtained in this study are compared to those known from experiments in Table 5.[81] The entries in Table 5 demonstrate excellent agreement between our simulations and experiments.

3.3. Model Validation. To test the derived parameters we performed a 200 ns MD simulation of a hydrated DPPC bilayer at 323 K for each of the six sets of parameters (Table 3). This particular temperature was selected because plenty of experimental data on the DPPC bilayer is available in the literature at this temperature. For model validation, three experimentally available bilayer parameters were used: (1) the surface area per lipid, which is only indirectly obtained from the experiment but is currently known with a high precision for DPPC; (2) the order parameter profile obtained from nuclear magnetic resonance spectroscopy; and (3) the X-ray scattering form factor. Additional parameters that characterize the lipid bilayer properties can be found in Supporting Information.

The first parameter to validate the computer model of the DPPC bilayer was the surface area per DPPC molecule, which was calculated by dividing the surface area of the simulation box by the number of DPPC molecules in a single bilayer leaflet. The area per lipid provides information about the bilayer phase state and is related to the ordering of the lipid acyl chains. Time evolution of the surface area per DPPC during 200 ns MD simulations of the all six bilayers (parameter sets, Table 3) is shown in Figure 6, together with the average values over the last 100 ns of the simulations. The surface area per DPPC obtained experimentally[82−84] is 0.63−0.64 nm^2; thus, only the DPPC model B4 (Table 3) closely reproduces the experimental values of the area per lipid (Figure 6). The other models underestimate the area by more than 0.1 nm^2. For this reason, the analyses below are carried out only for the model B4 (Table 3).

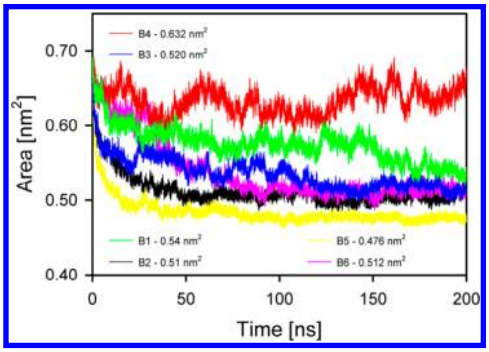

Figure 6. Time development of the surface area per DPPC in the bilayers studied with the six force field parameter sets (Table 3). For comparison, experimental values of the surface area[82−84] range 0.63−0.64 nm^2.

The deuterium order parameter, S_{CD},[85] is a lipid bilayer property that provides information about the lipid chain order. It can be obtained accurately from NMR experiments and is defined as

$$S_{CD} = \left\langle \frac{3}{2}(\cos^2 \theta i) - \frac{1}{2} \right\rangle \quad (2)$$

where θ_i is the angle between a C−D bond (C−H in simulations) of the ith carbon atom and the bilayer normal. The angular brackets denote averaging over time and over relevant C−D bonds in the bilayer. S_{CD} profiles, along both DPPC acyl chains obtained for the model B4 and along the DPPC *sn*-1 chain obtained experimentally,[86,87] are shown in Figure 7. The

Table 5. Densities and Heats of Vaporizations for Hydrocarbons Obtained in This Work and in Experimental (exp.) Studies[81]

	density kg/m^3	density exp. kg/m^3	Δdensity %	dH_{vap}	dH_{vap} (exp.)	.
C8	701.0 ± 0.1	698.6	0.3	40.12 ± 0.07	41.49	3
C12	752.6 ± 0.1	749.5	0.4	60.21 ± 0.07	61.52	2
C16	780.3 ± 0.1	770.1	1	80.78 ± 0.1	81.35	0.7

dx.doi.org/10.1021/jp5016627 | J. Phys. Chem. B 2014, 118, 4571−4581

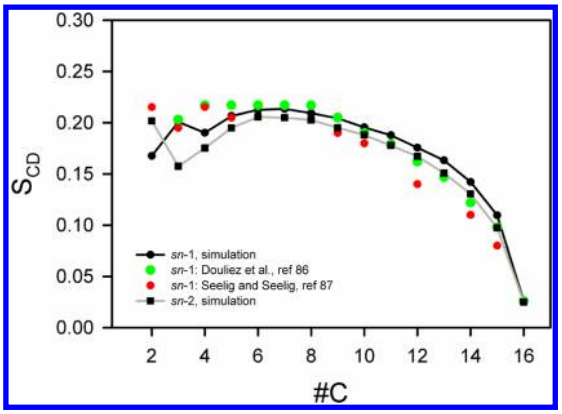

Figure 7. Profile of the S_{CD} order parameter for the *sn*-2 (square symbols, gray line) and *sn*-1 (black circle) chains obtained from MD simulations, and experimental data for the *sn*-1 hydrocarbon chains from refs 86 (green circle) and 87 (red circle).

profiles are close to one another, although some discrepancies are observed for carbons 2 and 3. Deuterium magnetic resonance studies demonstrated that the two C−D bonds of carbon 2 (C22, Figure 1) of the *sn*-2 chain are characterized by different values of S_{CD}, while in the case of the *sn*-1 chain (C32, Figure 1) the values are the same.[88] In our simulations, differences in the S_{CD} values of the C−D bonds in carbon 2 are observed in both chains (C22 and C32). Experimental and simulation values of the S_{CD} for the C−D bonds in the phosphatidylcholine and glycerol moieties are given in Table 6.

Table 6. $|S_{CD}|$ Values for Selected Carbons in the Phosphatidylcholine and Glycerol Moieties[a]

	α	β	g1		g2	g3	
experimental	0.05	0.04	0.00	0.13	0.2	0.21	0.23
simulation	0.04	0.05	0.01	0.17	0.2	0.13	0.23

[a]Experimental data are from refs 92−94. α refers to carbon 11, β to carbon 12, g1 to carbon 1, g2 to carbon 2, and g3 to carbon 3 in Figure 1.

The values obtained for the model B4 (Table 6) are in overall good agreement with experimental data; however, in the case of g3 (Table 6), there is a larger difference between orientations of two C−D bonds than what is observed experimentally.

The form factor, $F(q)$, computed from the simulations can be compared to experimental "model-free" measurements, since it is a primary quantity whose determination does not depend on assumptions during analysis. To get $F(q)$, first, the relative electron density profile $\rho_r(z)$ has to be computed by subtracting the electron density profile of the bulk water from that of the total system. The X-ray scattering form factor is then calculated as[82]

$$|F(q)| = \sqrt{\left(\int_{-L/2}^{L/2} \rho_r(z)\cos(qz)\,dz\right)^2 + \left(\int_{-L/2}^{L/2} \rho_r(z)\sin(qz)\,dz\right)^2} \quad (3)$$

where L is the length of the simulation box in the z direction. Form factors obtained in the MD simulations and experimentally[84] are shown in Figure 8.

In recent studies, Braun et al. (2013) performed a series of MD simulations of lipid bilayers to find out a dependence between the simulation box area and the calculated $F(q)$.[89] In each simulation, the box area is increased by 0.2 nm^2 per lipid

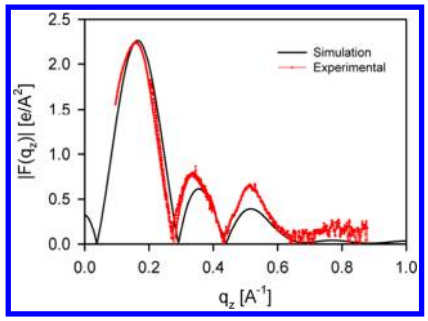

Figure 8. Absolute form factors as a function of the wavenumber q for the simulated DPPC bilayer model B4 (black). Comparison to experimental data (red) for a DPPC bilayer at 303 K taken from ref 84 indicates good agreement.

molecule, and the form factor is calculated and then compared with the experimental data. The obtained results allowed for the evaluation of the agreement between experimental and theoretical data. We used the same approach here. Based on the differences in the positions of the maxima in the lobes and the points where $F(q) = 0$ (Figure 8), which were obtained in this study and in experiment,[82] and the results of Braun et al. (2013),[89] one can conclude that the agreement between simulation and experiments is good. One can also conclude that the expected differences in surface areas per DPPC between experimental and theoretical values should be smaller than 0.02 nm^2.

Results of additional analyses for transmembrane density profiles, membrane thickness, volumes of lipids, chain tilt, and area and volume compressibility moduli are shown in Supporting Information and in ref 90.

4. CONCLUSIONS

In this study, an approach consistent with the OPLS-AA force field was used to recalculate torsional parameters, partial atomic charges, and some van der Waals (vdW) parameters for the polar part of a phosphatidylcholine molecule (headgroup and glycerol backbone), as well as torsional parameters for the PC hydrocarbon chains. To derive the new parameters, three quantum mechanical methods—Hartree−Fock, the second order Møller−Plesset perturbation theory, and the density functional theory—were used in vacuum and in a polar environment; for the latter, the Polarizable Continuum Model was employed. In effect, six parameter sets were generated. The new parameters were tested with simulations of a hydrated pure DPPC bilayer.

Out of the six tested sets, only for one (B4), generated using the MP2 method and PCM, was the surface area per DPPC within the range of the experimental values. This parameter set was further validated by comparisons of experimental and simulation data for deuterium order parameters and the X-ray form factor. The S_{CD} profiles along the DPPC *sn*-2 chain show overall good agreement with a small deviation at the beginning of the chain. Also, S_{CD} parameters calculated for the carbon atoms in the glycerol backbone and the choline moiety agree well with those obtained experimentally, with an exception for the g3 carbon atom, for which the difference between S_{CD} values for the two C−D bonds is higher in the simulation than in the experiment. Finally, agreement between form factors from the experiment and the present MD simulations is good.

The present study demonstrates that the computer model of DPPC is sensitive to even small differences in force-field

dx.doi.org/10.1021/jp5016627 | J. Phys. Chem. B 2014, 118, 4571−4581

parameters. The bilayer consisting of DPPC molecules parametrized with the B4 parameter set reproduces well the experimentally obtained data for a hydrated DPPC bilayer. Therefore, the approach used to generate this parameter set will be used in the future to develop OPLS-AA parameters for other lipids.

Small deviations between simulated and experimental data summarized above indicate that there is still space for further improvement in the force-field parameters. This might be achieved by using even more advanced quantum mechanical methods or by including additional terms in the potential function like the CMAP correction term[91] introduced to the CHARMM22 force field for proteins.

■ ASSOCIATED CONTENT

Supporting Information

Topology of DPPC in the Gromacs format with all necessary parameter files and structure of lipid bilayer in gro format; tables including torsional potentials derived from QM calculations; and additional results characterizing lipid bilayers (model B4). This material is available free of charge via the Internet at http://pubs.acs.org.

■ AUTHOR INFORMATION

Corresponding Author

*Tel.: +358 40 198 1010. Fax: +358 3 3115 3015. E-mail: tomasz.rog@tut.fi.

Notes

The authors declare no competing financial interest.

■ ACKNOWLEDGMENTS

We wish to thank the Academy of Finland for financial support (Center of Excellence in Biomembrane Research). I.V. thanks the European Research Council (Advanced Grant project CROWDED-PRO-LIPIDS). Financial support from the Polish Ministry of Science and Higher Education (PBZ-MniI-1/1/2005) is also acknowledged (M.P-G.). For computational resources, we wish to thank the CSC−IT Center for Science (Espoo, Finland) and ACK-Cyfronet, (Krakow, Poland).

■ REFERENCES

(1) Phillips, R.; Ursell, T.; Wiggins, P.; Sens, P. Emerging Roles for Lipids in Shaping Membrane-Protein Function. *Nature* **2009**, *459*, 379−385.

(2) Sundaralingam, M. Molecular Structures and Conformations of the Phospholipids and Sphingomyelins. *Ann. N. Y. Acad. Sci.* **1972**, *195*, 324−355.

(3) Berger, O.; Edholm, O.; Jahnig, F. Molecular Dynamics Simulations of a Fluid Bilayer of Dipalmitoylphosphatidylcholine at Full Hydration, Constant Pressure, and Constant Temperature. *Biophys. J.* **1997**, *72*, 2002−2013.

(4) Poger, D.; Mark, A. E. On the Validation of Molecular Dynamics Simulations of Saturated and *cis*-monounsaturated Phosphatidylcholine Lipid Bilayers: A Comparison with Experiment. *J. Chem. Theory Comput.* **2010**, *6*, 325−336.

(5) Kukol, A. Lipid Models for United-Atom Molecular Dynamics Simulations of Proteins. *J. Chem. Theory Comput.* **2009**, *5*, 615−626.

(6) Chandrasekhar, I.; Kastenholz, M.; Lins, R. D.; Oostenbrink, C.; Schuler, L. D.; Tieleman, D. P.; van Gunsteren, W. F. A Consistent Potential Energy Parameter Set for Lipids: Dipalmitoylphosphatidylcholine as a Benchmark of the GROMOS96 45A3 Force Field. *Eur. Biophys. J.* **2003**, *32*, 67−77.

(7) Chiu, S.-W.; Pandit, S. A.; Scott, H. L.; Jakobsson, E. An Improved United Atom Force Field for Simulation of Mixed Lipid Bilayers. *J. Phys. Chem. B* **2009**, *113*, 2748−2763.

(8) Smondyrev, A. M.; Berkowitz, M. L. United Atom Force Field for Phospholipid Membranes: Constant Pressure Molecular Dynamics Simulation of Dipalmitoylphosphatidicholine/Water System. *J. Comput. Chem.* **1999**, *20*, 531−545.

(9) Bhatnagar, N.; Kamath, G.; Potoff, J. J. Biomolecular Simulations with the Transferable Potentials for Phase Equilibria: Extension to Phospholipids. *J. Phys. Chem. B* **2013**, *117*, 9910−9921.

(10) Feller, S. E.; MacKerell, A. D., Jr. An Improved Empirical Potential Energy Function for Molecular Simulations of Phospholipids. *J. Phys. Chem. B* **2000**, *104*, 7510−7515.

(11) Sonne, J.; Jensen, M. Ø.; Hansen, F. Y.; Hemmingsen, L.; Peters, G. H. Reparameterization of All-Atom Dipalmitoylphosphatidylcholine Lipid Parameters Enables Simulation of Fluid Bilayers at Zero Tension. *Biophys. J.* **2007**, *92*, 4157−4167.

(12) Taylor, J.; Whiteford, N. E.; Bradley, G.; Watson, G. W. Validation of All-Atom Phosphatidylcholine Lipid Force Fields in the Tensionless NPT Ensemble. *Biochim. Biophys. Acta* **2009**, *1788*, 638−649.

(13) Klauda, J. B.; Venable, R. M.; Freites, J. A.; O'Connor, J. W.; Tobias, D. J.; Mondragon-Ramirez, C.; Vorobyov, I.; MacKerell, A. D., Jr.; Pastor, R. W. Update of the CHARMM All-Atom Additive Force Field for Lipids: Validation on Six Lipid Types. *J. Phys. Chem. B* **2010**, *114*, 7830−7843.

(14) Klauda, J. B.; Monje, V.; Kim, T.; Im, W. Improving the CHARMM Force Field for Polyunsaturated Fatty Acid Chains. *J. Phys. Chem. B* **2012**, *116*, 9424−9431.

(15) Lim, J. B.; Rogaski, B.; Klauda, J. B. Update of the Cholesterol Force Field Parameters in CHARMM. *J. Phys. Chem. B* **2012**, *116*, 203−210.

(16) Jojart, B.; Martinek, T. A. Performance of the General Amber Force Field in Modeling Aqueous POPC Membrane Bilayers. *J. Comput. Chem.* **2007**, *28*, 2051−2058.

(17) Siu, S. W. I.; Vácha, R.; Jungwirth, P.; Böckmann, R. A. Biomolecular Simulations of Membranes: Physical Properties from Different Force Fields. *J. Chem. Phys.* **2008**, *128*, 125103 1−12..

(18) Skjevik, A. A.; Madej, B. D.; Walker, R. C.; Teigen, K. LIPID11: A Modular Framework for Lipid Simulations Using Amber. *J. Phys. Chem. B* **2012**, *116*, 11124−11136.

(19) Dickson, C. J.; Madej, B. D.; Skjevik, Å. A.; Betz, R. M.; Teigen, K.; Gould, I. R.; Walker, R. C. Lipid14: The Amber Lipid Force Field. *J. Chem. Theory Comput.* **2014**, *10*, 865−879.

(20) Jämbeck, J. P. M.; Lyubartsev, A. P. Derivation and Systematic Validation of a Refined All-Atom Force Field for Phosphatidylcholine Lipids. *J. Phys. Chem. B* **2012**, *116*, 3164−3179.

(21) Jämbeck, J. P. M.; Lyubartsev, A. P. An Extension and Further Validation of an All-Atomistic Force Field for Biological Membranes. *J. Chem. Theory Comput.* **2012**, *8*, 2938−2948.

(22) Jämbeck, J. P. M.; Lyubartsev, A. P. Another Piece of the Membrane Puzzle: Extending Slipids Further. *J. Chem. Theory Comput.* **2013**, *9*, 774−784.

(23) Izvekov, S.; Voth, G. A. Multiscale Coarse-Graining of Mixed Phospholipid/Cholesterol Bilayer. *J. Chem. Theory Comput.* **2006**, *2*, 637−648.

(24) Bennuna, S. V.; Hoopesb, M. I.; Xingc, C.; Faller, R. Coarse-Grained Modeling of Lipids. *Chem. Phys. Lipids* **2009**, *159*, 59−66.

(25) Marrink, S. J.; Risselada, H. J.; Yefimov, S.; Tieleman, D. P.; de Vries, A. H. The MARTINI Force Field: Coarse Grained Model for Biomolecular Simulations. *J. Phys. Chem. B* **2007**, *111*, 7812−7824.

(26) Marrink, S. J.; Risselada, H. J.; Mark, A. E. Simulation of Gel Phase Formation and Melting in Lipid Bilayers Using a Coarse Grained Model. *Chem. Phys. Lipids* **2005**, *135*, 223−244.

(27) Risselada, H. J.; Marrink, S. J. The Molecular Face of Lipid Rafts in Model Membranes. *Proc. Natl. Acad. Sci. U.S.A.* **2008**, *105*, 17367−17372.

(28) Javanainen, M.; Hammaren, H.; Monticelli, L.; Jeon, J.-H.; Miettinen, M. S.; Martinez-Seara, H.; Metzler, R.; Vattulainen, I.

Anomalous and Normal Diffusion of Lipids and Proteins in Crowded Membranes. *Faraday Discuss.* **2012**, *161*, 397−417.
(29) Goose, J. E.; Sansom, M. S. P. Reduced Lateral Mobility of Lipids and Proteins in Crowded Membranes. *PLoS Comput. Biol.* **2013**, *9*, e1003033 1−10..
(30) Koivuniemi, A.; Vuorela, T.; Kovanen, P. T.; Vattulainen, I.; Hyvonen, M. Lipid Exchange Mechanism of the Cholesteryl Ester Transfer Protein Clarified by Atomistic and Coarse-Grained Simulations. *PLoS Comput. Biol.* **2012**, *8*, e1002299 1−9..
(31) Koivuniemi, A.; Vattulainen, I. High Density Lipoproteins: Revealing their Structural and Dynamical Properties through Molecular Simulations. *Soft Matter* **2012**, *8*, 1262−1267.
(32) Murtola, T.; Vuorela, T.; Hyvonen, M. T.; Marrink, S. J.; Karttunen, M.; Vattulainen, I. Low-Density Lipoprotein: Structure, Dynamics and Lipid − ApoB-100 Interactions. *Soft Matter* **2011**, *7*, 8135−8141.
(33) Rossi, G.; Ioannis, G.; Monticelli, L.; Rostedt, N. K. J.; Puisto, S. R.; Lowe, C.; Taylor, A. C.; Vattulainen, I.; Ala-Nissila, T. A MARTINI Coarse-Grained Model of a Thermoset Polyester Coating. *Macromolecules* **2011**, *44*, 6198−6208.
(34) Rossi, G.; Monticelli, L.; Puisto, S. R.; Vattulainen, I.; Ala-Nissila, T. Coarse-Graining Polymers with the MARTINI Force Field: Polysterene as a Benchmark Case. *Soft Matter* **2011**, *7*, 698−708.
(35) Bauer, B. A.; Patel, S. Recent Applications and Developments of Charge Equilibration Force Fields for Modeling Dynamical Charges in Classical Molecular Dynamics Simulations. *Theor. Chem. Acc.* **2012**, *131*, 1153−1159.
(36) Lucas, T. R.; Bauer, B. A.; Patel, S. Charge Equilibration Force Fields for Molecular Dynamics Simulations of Lpids, Bilayers, and Integral Membrane Protein Systems. *Biochim. Biophys. Acta* **2012**, *1818*, 318−329.
(37) Bauer, B. A.; Lucas, T. R.; Meninger, D. J.; Patel, S. Water Permeation through DMPC Lipid Bilayers Using Polarizable Charge Equilibration Force Fields. *Chem. Phys. Lett.* **2011**, *508*, 289−294.
(38) Chowdhary, J.; Harder, E.; Lopes, P. E. M.; Huang, L.; MacKerell, A. D., Jr.; Roux, B. A Polarizable Force Field of Dipalmitoylphosphatidylcholine Based on the Classical Drude Model for Molecular Dynamics Simulations of Lipids. *J. Phys. Chem. B* **2013**, *117*, 9142−9160.
(39) Jämbeck, J. P. M.; Lyubartsev, A. P. Implicit Inclusion of Atomic Polarization in Modeling of Partitioning Between Water and Lipid Bilayers. *Phys. Chem. Chem. Phys.* **2013**, *15*, 4677−4686.
(40) Jorgensen, W. L.; Maxwell, D. S.; TiradoRives, J. Development and Testing of the OPLS All-Atom Force Field on Conformational Energetics and Properties of Organic Liquids. *J. Am. Chem. Soc.* **1996**, *118*, 11225−11236.
(41) Kaminski, G. A.; Friesner, R. A.; Tirado-Rives, J.; Jorgensen, W. L. Evaluation and Reparametrization of the OPLS-AA Force Field for Proteins via Comparison with Accurate Quantum Chemical Calculations on Peptides. *J. Phys. Chem.* **2001**, *105*, 6474−6487.
(42) Guimaraes, C. R. W.; Boger, D. L.; Jorgensen, W. L. Elucidation of Fatty Acid Amide Hydrolase Inhibition by Potent Alpha-Ketoheterocycle Derivatives from Monte Carlo Simulations. *J. Am. Chem. Soc.* **2005**, *127*, 17377−17384.
(43) Ulmschneider, J. P.; Jorgensen, W. L. Monte Carlo Backbone Sampling for Nucleic Acids Using Concerted Rotations Including Variable Bond Angles. *J. Phys. Chem. B* **2004**, *108*, 16883−16892.
(44) Damm, W.; Frontera, A.; TiradoRives, J.; Jorgensen, W. L. OPLS All-Atom Force Field for Carbohydrates. *J. Comput. Chem.* **1997**, *18*, 1955−1970.
(45) Carlson, H. A.; Masukawa, K. M.; Rubins, K.; Bushman, F. D.; Jorgensen, W. L.; Lins, R. D.; Briggs, J. M.; McCammon, J. A. Developing a Dynamic Pharmacophore Model for HIV-1 Integrase. *J. Med. Chem.* **2000**, *43*, 2100−2114.
(46) Lamb, M. L.; Jorgensen, W. L. Investigations of Neurotrophic Inhibitors of FK506 Binding Protein via Monte Carlo Simulations. *J. Med. Chem.* **1998**, *41*, 3928−3939.
(47) Jorgensen, W. L. The Many Roles of Computation in Drug Discovery. *Science* **2004**, *303*, 1813−1818.
(48) Duffy, E. M.; Jorgensen, W. L. Prediction of Properties from Simulations: Free Energies of Solvation in Hexadecane, Octanol, and Water. *J. Am. Chem. Soc.* **2000**, *122*, 2878−2888.
(49) Siu, S. W. I.; Pluhackova, K.; Böckmann, R. A. Optimization of the OPLS-AA Force Field for Long Hydrocarbons. *J. Chem. Theory Comput.* **2012**, *8*, 1459−1470.
(50) Murzyn, K.; Bratek, M.; Pasenkiewicz-Gierula, M. Refined OPLS All-Atom Force Field Parameters for n-Pentadecane, Methyl Acetate, and Dimethyl Phosphate. *J. Phys. Chem. B* **2013**, *117*, 16388−16396.
(51) Pasenkiewicz-Gierula, M.; Róg, T.; Kitamura, K.; Kusumi, A. Cholesterol Effects on the Phosphatidylcholine Bilayer Polar Region: A Molecular Simulation Study. *Biophys. J.* **2000**, *78*, 1376−1389.
(52) Róg, T.; Pasenkiewicz-Gierula, M. Cholesterol Effects on the Pchosphatidylcholine Bilayer Nonpolar Region: A Molecular Simulation Study. *Biophys. J.* **2001**, *81*, 2190−2202.
(53) Orłowski, A.; Bunker, A.; Pasenkiewicz-Gierula, M.; Vattulainen, I.; Männistö, P. T.; Róg, T. Strong Preferences of Dopamine and L-dopa Towards Lipid Head Group: Importance of Phosphatidylserine and its Implication for Neurotransmitters Metabolism. *J. Neurochem.* **2012**, *122*, 681−690.
(54) Stępniewski, M.; Kepczynski, M.; Jamróz, D.; Nowakowska, M.; Rissanen, S.; Vattulainen, I.; Róg, T. Interaction of Hematoporphyrin with Lipid Bilayer. Molecular Dynamics Simulation Studies. *J. Chem. Phys. B* **2012**, *116*, 4889−4897.
(55) Magarkar, A.; Karakas, E.; Stepniewski, M.; Róg, T.; Bunker, A. Molecular Dynamics Simulation of PEGylated Bilayer Interacting with Salt Ions: a Model of the Liposome Surface in the Bloodstream. *J. Phys. Chem. B* **2012**, *116*, 4212−4219.
(56) Krishnamurty, S.; Stefanov, M.; Mineva, T.; Bégu, S.; Devoisselle, J. M.; Goursot, A.; Zhu, R.; Salahub, D. R. Density Functional Theory-Based Conformational Analysis of a Phospholipid Molecule (Dimyristoyl Phosphatidylcholine). *J. Phys. Chem. B* **2008**, *112*, 13433−13442.
(57) Jorgensen, W. L.; Chandrasekhar, J.; Madura, J. D.; Impey, R. W.; Klein, M. L. Comparison of Simple Potential Functions for Simulating Liquid Water. *J. Chem. Phys.* **1983**, *79*, 926−935.
(58) Hess, B.; Kutzner, C.; van der Spoel, D.; Lindahl, E. GROMACS 4: Algorithms for Highly Efficient, Load-Balanced, and Scalable Molecular Simulation. *J. Chem. Theory Comput.* **2008**, *4*, 435−447.
(59) Becke, A. D. Density-Functional Thermochemistry. III. The Role of Exact Exchange. *J. Chem. Phys.* **1993**, *98*, 5648−5652.
(60) Aissing, G.; Monkhorst, H. J. Linear Dependence in Basis-Set Calculations for Extended Systems. *Int. J. Quantum Chem.* **1992**, *43*, 733−745.
(61) Frisch, M. J.; Trucks, G. W.; Schlegel, H. B.; Scuseria, G. E.; Robb, M. A.; Cheeseman, J. R.; Montgomery, J. A.; Vreven, T., Jr.; Kudin, K. N.; Burant, J. C. et al. *Gaussian 03*, revision C.02; Gaussian, Inc.: Wallingford, CT, 2004.
(62) Cossi, M.; Scalmani, G.; Rega, N.; Barone, V. New Developments in the Polarizable Continuum Model for Quantum Mechanical and Classical Calculations on Molecules in Solution. *J. Chem. Phys.* **2002**, *117*, 43−54.
(63) Yang, L. J.; Tan, C. H.; Hsieh, M. J.; Wang, J. M.; Duan, Y.; Cieplak, P.; Caldwell, J.; Kollman, P. A.; Luo, R. New-Generation Amber United-Atom Force Field. *J. Phys. Chem. B* **2006**, *110*, 13166−13176.
(64) Mládek, A.; Krepl, M.; Svozil, D.; Cech, P.; Otyepka, M.; Banáš, P.; Zgarbová, M.; Jurečka, P.; Sponer, J. Benchmark Quantum-Chemical Calculations on a Complete Set of Rotameric Families of the DNA Sugar-Phosphate Backbone and Their Comparison with Modern Density Functional theory. *Phys. Chem. Chem. Phys.* **2013**, *15*, 7295−7310.
(65) Pluharova, E.; Oncak, M.; Seidel, R.; Schroeder, C.; Schroeder, W.; Winter, B.; Bradforth, S. E.; Jungwirth, P.; Slavícek, P. Transforming Anion Instability into Stability: Contrasting. Photoionization of Three Protonation Forms of the Phosphate Ion upon Moving into Water. *J. Phys. Chem. B* **2012**, *116*, 13254−13264.

(66) Breneman, C. M.; Wiberg, Ke. B. Determining Atom-Centered Monopoles from Molecular Electrostatic Potentials. The Need for High Sampling Density in Formamide Conformational analysis. *J. Comput. Chem.* **1990**, *11*, 361−373.
(67) Dupradeau, F.-Y.; Pigache, A.; Zaffran, T.; Savineau, C.; Lelong, R.; Grivel, N.; Lelong, D.; Rosanski, W.; Cieplak, P. The R.E.D. Tools: Advances in RESP and ESP Charge Derivation and Force Field Library Building. *Phys. Chem. Chem. Phys.* **2010**, *12*, 7821−7839.
(68) Bayly, C. I.; Cieplak, P.; Cornell, W.; Kollman, P. A. A Well-Behaved Electrostatic Potential Based Method Using Charge Restraints for Deriving Atomic Charges: The RESP Model. *J. Phys. Chem.* **1993**, *97*, 10269−10280.
(69) Cornell, W. D.; Cieplak, P.; Bayly, C. I.; Kollmann, P. A. Application of RESP Charges to Calculate Conformational Energies, Hydrogen Bond Energies, and Free Energies of Solvation. *J. Am. Chem. Soc.* **1993**, *115*, 9620−9631.
(70) Levenberg, K. A Method for the Solution of Certain Non-Linear Problems in Least Squares. *Q. Appl. Math.* **1944**, *2*, 164−168.
(71) Williams, T.; Kelley, C. *Gnuplot 4.2*, An Interactive Plotting Program.
(72) Klauda, J. B.; Garrison, S. L.; Arora, G.; Jiang, J.; Sandler, S. I. HM-IE: A Quantum Chemical Hybrid Method for Accurate Interaction Energies. *J. Phys. Chem. A* **2004**, *108*, 107−112.
(73) Klauda, J. B.; Brooks, B. R.; MacKerell, A. D.; Venable, R. M.; Pastor, R. W. An Ab Initio Study on the Torsional Surface of Alkanes and its Effect on Molecular Simulations of Alkanes and DPPC Bilayers. *J. Phys. Chem. B* **2005**, *109*, 5300−5311.
(74) Róg, T.; Bunker, A.; Vattulainen, I.; Karttunen, M. Effect of Glucose and Galactose Headgroup on Lipid Bilayer Properties. *J. Phys. Chem. B* **2007**, *111*, 10146−10154.
(75) Essman, U.; Perera, L.; Berkowitz, M. L.; Darden, H. L. T.; Pedersen, L. G. A Smooth Particle Mesh Ewald Method. *J. Phys. Chem.* **1995**, *103*, 8577−8592.
(76) Hess, B.; Bekker, H.; Berendsen, H. J. C.; Fraaije, J. G. E. M. LINCS: A Linear Constraint Solver for Molecular Simulations. *J. Comput. Chem.* **1997**, *18*, 1463−1472.
(77) Nose, S. A Unified Formulation of the Constant Temperature Molecular Dynamics Methods. *J. Chem. Phys.* **1984**, *81*, 511−519.
(78) Hoover, W. G. Canonical Dynamics: Equilibrium Phase-Space Distributions. *Phys. Rev. A* **1985**, *31*, 1695−1697.
(79) Parrinello, M.; Rahman, A. Polymorphic Transitions in Single Crystals: A New Molecular Dynamics Method. *J. Appl. Phys.* **1981**, *52*, 7182−7190.
(80) Akutsu, H. Direct Determination by Raman Scattering of the Conformation of the Choline Group in Phospholipid Bilayers. *Biochemistry* **1981**, *20*, 7359−7366.
(81) Lide, D. R., Ed. *CRC Handbook of Chemistry and Physics*, 90th ed.; CRC Press (Taylor and Francis Group): Boca Raton, FL, 2009.
(82) Nagle, J. F.; Zhang, R.; Tristram-Nagle, S.; Sun, W.; Petrache, H. I.; Suter, R. M. X-Ray Structure Determination of Fully Hydrated L. Phase Dipalmitoylphosphatidylcholine Bilayers. *Biophys. J.* **1996**, *70*, 1419−1431.
(83) Petrache, H. I.; Dodd, S. W.; Brown, M. F. Area per Lipid and Acyl Length Distributions in Fluid Phosphatidylcholines Determined by 2H NMR Spectroscopy. *Biophys. J.* **2000**, *79*, 3172−3192.
(84) Kucerka, N.; Tristram-Nagle, S.; Nagle, J. F. Closer Look at Structure of Fully Hydrated Fluid Phase DPPC Bilayers. *Biophys. J.* **2006**, *90*, L83−L85.
(85) Davis, J. H. The Description of Membrane Lipid Conformation, Order and Dynamics by ^{2}H-NMR. *Biochim. Biophys. Acta* **1983**, *737*, 117−171.
(86) Douliez, J.-P.; Leonard, A.; Dufourc, E. J. Restatement of Order Parameters in Biomembranes: Calculation of C-C Bond Order Parameters from C-D Quadrupolar Splittings. *Biophys. J.* **1995**, *68*, 1727−1739.
(87) Seelig, A.; Seelig, J. The Dynamic Structure of Fatty Acyl Chains in a Phospholipid Bilayer Measured by Deuterium Magnetic Resonance. *Biochemistry* **1974**, *13*, 4839−4845.
(88) Seelig, A.; Seelig, J. Bilayers of Dipalmitoyl-3-sn-Phosphatidylcholine conformational Differences between the Fatty Acyl Chains. *Biochim. Biophys. Acta* **1975**, *406*, 1−5.
(89) Braun, A. R.; Sachs, J. N.; Nagle, J. F. Comparing Simulations of Lipid Bilayers to Scattering Data: The GROMOS 43A1-S3 Force Field. *J. Phys. Chem. B* **2013**, *117*, 5065−5072.
(90) Kulig, W.; Tynkkynen, J.; Javanainen, M.; Manna, M.; Rog, T.; Vattulainen, I.; Jungwirth, P. How Well does Cholesteryl Hemisuccinate Mimic Cholesterol in Saturated Phospholipid Bilayers? *J. Mol. Modeling* **2014**, *20*, 2121 1−9.
(91) Buck, M.; Bouguet-Bonnet, S.; Pastor, R. W.; MacKerell, A. D., Jr. Importance of the CMAP Correction to the CHARMM22 Protein Force Field: Dynamics of Hen Lysozyme. *Biophys. J.* **2006**, *15*, L36−L38.
(92) Seelig, J.; Gally, H.; Wohlgemuth, R. Orientation and Flexibility of the Choline Head Group in Phosphatidylcholine Bilayers. *Biochim. Biophys. Acta* **1977**, *467*, 109−119.
(93) Gross, J. D.; Warchawski, D. E.; Griffin, R. G. Dipolar Recoupling in MAS NMR: A Probe for Segmental Order in Lipid Bilayers. *J. Am. Chem. Soc.* **1997**, *119*, 796−802.
(94) Mendes Ferreira, T.; Coreta-Gomes, F.; Ollila, O. H. S.; Moreno, M. J.; Vaz, W. L. C.; Topgaard, D. Cholesterol and POPC Segmental Order Parameters in Lipid Membranes: Solid State 1H−13C NMR and MD Simulation Studies. *Phys. Chem. Chem. Phys.* **2013**, *15*, 1976−1989.